THE JOURNAL OF BIOLOGICAL CHEMISTRY VOL. 281, NO. 9, pp. 5416–5425, March 3, 2006

Quantitative Analysis of Muscarinic Acetylcholine Receptor Homo- and Heterodimerization in Live Cells

REGULATION OF RECEPTOR DOWN-REGULATION BY HETERODIMERIZATION[*][S]

Received for publication, July 11, 2005, and in revised form, November 22, 2005 Published, JBC Papers in Press, December 20, 2005, DOI 10.1074/jbc.M507476200

Juan C. Goin[‡1] **and Neil M. Nathanson**[§2]

From the [‡]*Centro de Estudios Farmacológicos y Botánicos, Consejo Nacional de Investigaciones Científicas y Técnicas, Buenos Aires 1414, Argentina and the* [§]*Department of Pharmacology, University of Washington School of Medicine, Seattle, Washington 98195*

Although previous pharmacological and biochemical data support the notion that muscarinic acetylcholine receptors (mAChR) form homo- and heterodimers, the existence of mAChR oligomers in live cells is still a matter of controversy. Here we used bioluminescence resonance energy transfer to demonstrate that M_1, M_2, and M_3 mAChR can form constitutive homo- and heterodimers in living HEK 293 cells. Quantitative bioluminescence resonance energy transfer analysis has revealed that the cell receptor population in cells expressing a single subtype of M_1, M_2, or M_3 mAChR is predominantly composed of high affinity homodimers. Saturation curve analysis of cells expressing two receptor subtypes demonstrates the existence of high affinity M_1/M_2, M_2/M_3, and M_1/M_3 mAChR heterodimers, although the relative affinity values were slightly lower than those for mAChR homodimers. Short term agonist treatment did not modify the oligomeric status of homo- and heterodimers. When expressed in JEG-3 cells, the M_2 receptor exhibits much higher susceptibility than the M_3 receptor to agonist-induced down-regulation. Coexpression of M_3 mAChR with increasing amounts of the M_2 subtype in JEG-3 cells resulted in an increased agonist-induced down-regulation of M_3, suggesting a novel role of heterodimerization in the mechanism of mAChR long term regulation.

Over the last decade, many studies have shown broad evidence that G protein-coupled receptors (GPCR)[3] interact with one another to form constitutive homo- or hetero-oligomers. GPCR dimerization has been implicated in many aspects of receptor pharmacology, such as maturation, ligand binding, activation, signaling, desensitization, endocytosis, and trafficking (1–3). In the early 1990s, several studies showed that muscarinic acetylcholine receptors (mAChR), like other GPCR, might be arranged in dimeric or oligomeric complexes. Complex binding curves for both muscarinic agonists and antagonists were interpreted as evidence for the existence of multiple states of affinity, which is consistent with the notion of binding sites located on dimeric receptor molecules (4, 5). More recent studies on mAChR have shown that such heterogeneity of affinity should rather be attributed to nucleotide-sensitive cooperative effects between interacting sites (6, 7). Because there seems to be one binding site per receptor molecule, cooperativity suggests that mAChR are actually oligomers formed by two or more interacting sites (6).

Additional pharmacological evidence that mAChR can form dimers was provided by Maggio *et al.* (8), who used chimeric α_2-adrenergic/M_3 muscarinic receptors composed of the first five transmembrane domains (TMD) of one receptor and the last two TMD of the other. No binding or signaling was detected when either fusion protein was expressed alone, but coexpression of both chimeras rescued binding activity and signaling properties of both adrenergic and muscarinic ligands. These results were interpreted as intermolecular interactions between two inactive receptors now engaged in a dimeric complex with restored receptor functional properties. However, such trans-complementation results have been challenged because of the fact that those intermolecular interactions were seen by studying mutant receptors and not wild type receptors (1). Coimmunoprecipitation of solubilized epitope-tagged M_3 mAChR and Western blot analysis has also been employed to demonstrate the existence of mAChR oligomers in a direct fashion. This biochemical approach revealed that the M_3 mAChR is capable of forming disulfide-linked as well as noncovalent dimers/multimers (9). Although coimmunoprecipitation/immunoblotting assays provide fairly convincing evidence for mAChR dimer formation, such studies have been criticized for the possibility that the observed receptor aggregation could result from an artifact because of the presence of concentrated preparations of highly hydrophobic molecules following the solubilization process (1). Over the last decade, several groups have used biophysical assays based on light resonance energy transfer to assess GPCR oligomerization (1, 2, 10, 11). Fluorescence resonance energy transfer and its variation, bioluminescence resonance energy transfer (BRET), have been used extensively to overcome technological limitations present in pharmacological and biochemical methods because they have the distinct advantage of monitoring real time interactions between proteins synthesized in their correct location in living cells (10). In the classical BRET methodology, the first protein is fused to *Renilla* luciferase (*R*Luc), and the second protein partner is fused to a fluorescent protein (yellow fluorescent protein (YFP)). If both partners interact, resonance energy transfer between *R*Luc (donor) and the YFP (acceptor) can be measured upon addition of the *R*Luc substrate coelenterazine (12).

In this study, the occurrence of constitutive homo- and hetero-oligomers among M_1, M_2, and M_3 mAChR was investigated in living cells expressing physiological levels of these receptors by BRET. BRET satu-

* This work was supported by National Institutes of Health Grants NS26920 and HL44948 and by grants from the Pew Latin American Program for the Biomedical Sciences and Fundación Antorchas. The costs of publication of this article were defrayed in part by the payment of page charges. This article must therefore be hereby marked "*advertisement*" in accordance with 18 U.S.C. Section 1734 solely to indicate this fact.

[S] The on-line version of this article (available at http://www.jbc.org) contains supplemental Figs. 1–4.

[1] Researcher for Consejo Nacional de Investigaciones Científicas y Técnicas.

[2] To whom correspondence should be addressed: Dept. of Pharmacology, University of Washington, Box 357750, Seattle, WA 98195-7750. Tel.: 206-543-9457; Fax: 206-616-4230; E-mail: nathanso@u.washington.edu.

[3] The abbreviations used are: GPCR, G protein-coupled receptor; mAChR, muscarinic acetylcholine receptor; TMD, transmembrane domain; BRET, bioluminescence resonance energy transfer; *R*Luc, *Renilla* luciferase; YFP, yellow fluorescence protein, GFP, green fluorescence protein; Smo, smoothened; QNB, quinuclidinyl benzilate; i3, third intracellular loop; PBS, phosphate-buffered saline; HA, hemagglutinin.

ration experiments were conducted to estimate the relative ability of each receptor subtype to engage in homo- and heterotropic interactions. The nature of such homo-oligomers, the proportion of receptor molecules forming those oligomeric complexes, and the effect of muscarinic agonist on M_1, M_2, and M_3 mAChR homo- and heterodimerization were also addressed. Finally, we examined the implications of oligomerization on mAChR function by determining the effect of M_2/M_3 heterodimerization on agonist-induced M_3 mAChR regulation.

EXPERIMENTAL PROCEDURES

Materials—[^{3}H]Quinuclidinyl benzilate ([^{3}H]QNB, 42 Ci/mmol) and *N*-[^{3}H]methylscopolamine (81 Ci/mmol) were purchased from Amersham Biosciences. Dulbecco's modified Eagle's medium, penicillin/streptomycin, and fetal bovine serum were purchased from Invitrogen. Restriction enzymes were from New England Biolabs (Beverly, MA), and coelenterazine h was obtained from Promega (Madison, WI). The anti-HA polyclonal antibody (HA.11) was purchased from Covance (Berkeley, CA). Carbamylcholine chloride (carbachol), atropine sulfate, anti-FLAG M2 monoclonal antibody, and all other reagents were purchased from Sigma. The monoclonal antibody against the porcine cardiac M_2 mAChR was generated and characterized by Luetje *et al.* (13).

Receptor Constructs—mAChR-*R*Luc and mAChR-YFP fusion proteins were constructed by ligating the *Renilla* luciferase (*R*Luc) and the YFP moieties to the C-terminal end of the receptors. Mouse M_1, porcine M_2, and human M_3 mAChR coding sequences without their stop codons were amplified by using sense and antisense primers harboring unique restriction sites. The fragments were then subcloned in-frame into pRL-CMV-*R*Luc (Promega) or pEYFP-N1 (Clontech, Palo Alto, CA). Restriction sites used were as follows: XhoI/BamHI (M_1-*R*Luc, M_1-YFP), XhoI/SacII (M_2-*R*Luc, M_2-YFP), EcoRV/BamHI (M_3-*R*Luc), and EcoRI/BamHI (M_3-YFP). pEYFP was cut with AgeI and BsrGI, and the YFP fragment was inserted into the AgeI/BsrGI site from human Smoothened-GFP (Smo-GFP) to give Smo-YFP. Smo-GFP was provided by Dr. A. Kaykas (University of Washington). The HA-M_3 mAChR expression plasmid was obtained from University of Missouri-Rolla cDNA Resource Center (Rolla, MO). All other constructs have been described elsewhere (14, 15).

Cell Culture and Transfection—HEK 293 or JEG-3 cells were grown in Dulbecco's modified Eagle's medium supplemented with 10% (v/v) fetal bovine serum and penicillin (100 units/ml)/streptomycin sulfate (0.1 mg/ml) at 37 °C in a humidified 10% CO_2 environment. Transient transfections were performed on cells that were at 70–80% confluence using the calcium phosphate precipitation protocol (16).

Pharmacological Characterization of Constructs—HEK 293 cells grown in 15-cm dishes were transfected with *R*Luc-tagged, YFP-tagged, or nontagged mAChR (12.5-25 μg of DNA/plate). Following a 36-h period post-transfection, cells were washed with ice-cold PBS, and membranes were obtained as described previously (17). Saturation binding studies were performed by incubating membranes with increasing concentrations of [^{3}H]QNB at 37 °C for 90 min in 50 mM sodium/potassium phosphate, pH 7.4. Atropine (1 μM) was used to define nonspecific binding. The reaction was stopped by rapid filtration over GF/C glass-fiber filters (Whatman). Filters were then washed four times with cold phosphate buffer, and the retained radioactivity was determined by scintillation counting. Curves were analyzed by nonlinear regression analysis using Prism 4 software (GraphPad, San Diego).

BRET Assays—Thirty six hours after transfection, HEK 293 cells were distributed in 96-well microplates (white opaque Isoplate, Wallac) washed with phosphate-buffered saline (PBS) and resuspended in PBS/glucose 0.1% in the presence or absence of 10 μM carbachol at 25 °C. Coelenterazine h was added at a final concentration of 5 μM, and light intensity was sequentially integrated in the 510–590 and 440–500 nm windows using a Victor^2 multiplate reader (PerkinElmer Life Sciences). BRET ratio was defined as ((emission at 510–590)/(emission at 440–500)) − *Cf*, where *Cf* corresponded to (emission at 510–590)/(emission at 440–500) for the receptor *R*Luc constructs expressed alone in the same experiments.

Fluorescence and Luminescence Measurements—Transiently transfected HEK 293 cells were harvested, washed, and resuspended as described above and then distributed in 96-well microplates (either clear-bottomed or white opaque Isoplates for fluorescence and luminescence determinations, respectively). Both determinations were also carried out in a Victor^2 multiplate reader. The total fluorescence of cells was measured using an excitation filter of 485 nm and an emission filter of 535 nm. For assessing the activity of *Renilla* luciferase, total luminescence was determined on samples incubated with 5 μM coelenterazine. For both measurements, the means of duplicate wells were calculated. Total fluorescence values were then divided by the background determined in wells containing untransfected cells. The background values for total luminescence were negligible, and they were subtracted from sample values.

Titration of Donor and Acceptor Fusion Proteins—Expression levels of mAChR-*R*Luc and mAChR-YFP constructs were monitored by measuring luminescence and fluorescence, respectively, as described above. This procedure is based on the observation that luminescence and fluorescence levels of several receptor-*R*Luc and receptor-YFP (or receptor-GFP) fusion proteins have been found to be linearly correlated with receptor numbers (18). Because this correlation is an intrinsic property of each fusion protein, we tested whether our mAChR fusion proteins followed a linear correlation pattern. Thus, we expressed each mAChR-*R*Luc or mAChR-YFP at different levels in HEK 293 cells and assessed the relationship between luciferase activity or fluorescence, respectively, and the amount of mAChR-binding sites in the same cells. Thirty six hours after transfection, ~20,000 HEK 293 cells were incubated with 1 nM [^{3}H]QNB in PBS, 0.1% glucose for 90 min at 25 °C. Nonspecific binding was determined in the presence of 1 μM atropine. The reaction was stopped by rapid filtration over GF/C glass-fiber filters, which were then washed four times with cold PBS. Retained radioactivity was determined as described above. Luminescence and fluorescence (arbitrary units) were plotted against total binding sites, and linear regression curves were obtained (supplemental Fig. 2). These standard curves generated for each single experiment were used to transform fluorescence and luminescence values into femtomoles of receptor. Thus, the fluorescence/luminescence ratios were transformed into (receptor-YFP)/(receptor-*R*Luc) ratios, which allowed us to determine accurate $BRET_{max}$ and $BRET_{50}$ values (19). Protein concentration of samples was determined to control for the number of cells and also to express receptor numbers in femtomole/mg of total cell protein, using the standard method described by Lowry *et al.* (20).

Receptor Down-regulation Assays—Determination of agonist-induced M_2 or M_3 mAChR down-regulation was accomplished using the binding of the membrane-permeable muscarinic ligand [^{3}H]QNB to intact cells expressing either mAChR subtype, as described previously (21). Briefly, JEG-3 cells were transiently transfected with either M_2 or FLAG-M_3 mAChR DNA constructs. Forty eight hours later cells were incubated either with 1 mM carbachol for different times (within a 0–12-h-range) or in the presence of various concentrations of carbachol for 12 h at 37 °C. Cells were then washed with ice-cold PBS and labeled with a saturating concentration of [^{3}H]QNB (~1 nM) in PBS for 90 min at 37 °C. Nonspecific binding was determined in the presence of

1 μM atropine. Labeled cells were washed with ice-cold PBS and filtered onto GF/C membrane filters (Whatman). Filters were then washed with ice-cold PBS, transferred to scintillation vials, and combined with scintillation fluid before the determination of radioactivity by scintillation counting.

Down-regulation of Coexpressed M_2 and M_3 mAChR—JEG-3 cells were transfected with M_2 mAChR, FLAG-M_3 mAChR, or both DNA constructs at different proportions following the procedure indicated above. Forty eight hours post-transfection, cells were treated with 10 μM carbachol for 12 h at 37 °C. Cells were then washed with ice-cold PBS, harvested in 50 mM sodium/potassium phosphate buffer, pH 7.4, supplemented with protease inhibitors (10 μg/ml leupeptin, 70 μg/ml phenylmethanesulfonyl fluoride, and 0.25 μg/ml pepstatin A), and were glass-glass homogenized. Membranes were obtained as described previously (17), and the total number of mAChR in crude membrane homogenates was determined using the binding of [^{3}H]QNB as described by Halvorsen and Nathanson (22). The numbers of M_2 and FLAG-M_3 mAChR were measured by the immunoprecipitation assay described previously (23) using anti-M_2 and anti-FLAG monoclonal antibodies, respectively.

Alternatively, control experiments were performed by cotransfecting cells with FLAG-M_3 mAChR and HA-M_3 mAChR at different relative expression levels, as determined by immunoprecipitation using anti-FLAG and anti-HA antibodies (23). The extent of FLAG-M_3 down-regulation after carbachol treatment was then determined as indicated above.

Data Analysis—BRET saturation curves were analyzed using Prism 4 software. Isotherms were fitted using a nonlinear regression equation assuming a single binding site, which provided $BRET_{max}$ and $BRET_{50}$ values. The correlation between fluorescence or luminescence and receptor density was analyzed by linear regression curve fitting with the same software. Statistical significance of differences in M_2 *versus* M_3 mAChR regulation was assessed by the two-tailed unpaired Student's *t* test.

RESULTS

Homo- and heterodimerization of M_1, M_2, and M_3 mAChR were assessed in live HEK 293 cells by quantitative BRET analysis. For this purpose, the three mAChR subtypes were fused at their C terminus to the energy donor *R*Luc or the acceptor YFP. To ensure that the expressed fusion proteins were properly folded polypeptides capable of binding muscarinic ligands, we assessed their binding properties by saturation binding assays using the muscarinic antagonist [^{3}H]QNB. Detailed analysis of the K_d values obtained from those saturation curves (Table 1) indicated that the modifications at the C terminus of M_1, M_2, and M_3 mAChR did not significantly alter the affinity for the muscarinic radioligand as compared with the wild type receptors. In another set of experiments, all constructs were individually expressed in HEK 293 cells, and the binding of the membrane-impermeable muscarinic ligand *N*-[^{3}H]methylscopolamine was determined in parallel with the binding of the membrane-permeable muscarinic antagonist [^{3}H]QNB at saturating radioligand concentrations for each receptor expressed. Because no significant difference was found between the binding levels of both radioligands to the same receptor,[4] we concluded that all fusion proteins are expressed at the cell surface and that such colocalization ensures their chances of interacting with each other.

To determine whether M_1, M_2, and M_3 mAChR can form homodimers in intact cells, we assessed the ability of coexpressed *R*Luc-tagged mAChR and YFP-tagged mAChR to interact with one another by BRET saturation curve analysis. HEK 293 cells were transiently cotransfected with a constant amount of the *R*Luc construct and increasing amounts of the YFP construct, and the transfer of energy between both fusion proteins was measured upon addition of the *Renilla* luciferase substrate coelenterazine h. The expression levels of each *R*Luc-tagged receptor were assessed by detection of total luminescence from the previous luciferase reaction, and the expression levels of the YFP-tagged receptors were monitored by determination of total fluorescence. Because the expression levels of *R*Luc constructs were found to be modified by the cotransfection of increasing amounts of their YFP partners, BRET signals were plotted as a function of the fluorescence/luminescence ratio. Coexpression of M_1, M_2, or M_3 donor molecules with their homologous acceptor partners resulted in classical saturation isotherms (Fig. 1, *A–C*), in which BRET signals increased as a hyperbolic function of the concentration of the acceptor, reaching an asymptote that corresponds to the saturation of all BRET donors by acceptor molecules. This observation suggests that M_1, M_2, and M_3 mAChR form constitutive homodimers in live cells. To ensure that these BRET signals did not result from a spurious interaction between *R*Luc and YFP, we performed control assays in which each *R*Luc-tagged mAChR was coexpressed with increasing amounts of soluble YFP. These saturation assays resulted in quasi-linear curves showing marginal BRET signals, which indicate a nonspecific interaction between both coexpressed partners in each case. The selectivity of the interaction between donor and acceptor mAChR was further assessed to rule out the possibility of nonspecific BRET signals because of transmembrane protein overexpression. The distantly related seven transmembrane signaling receptor Smoothened fused to YFP (Smo-YFP) was cotransfected with M_1, M_2, or M_3 mAChR-*R*Luc, which resulted in a dramatically decreased BRET ratio for the three mAChR tested. In contrast, coexpression of Smo-*R*Luc with increasing amounts of Smo-YFP yielded significantly higher BRET levels (supplemental Fig. 1), indicating that Smo-*R*Luc is effectively capable of forming constitutive dimers in intact cells when coexpressed with a specific partner. BRET data were not influenced by the relative position of *R*Luc or YFP on the receptor pairs because identical results were obtained for the reciprocal orientation.[4] These data confirm our previous observation, indicating that M_1, M_2, and M_3 donor and acceptor fusion proteins are engaged in specific interactions as constitutive homodimers.

Although the saturation curves shown previously suggest that M_1, M_2, and M_3 donor and acceptor specifically interact with each other, they do not provide enough information about the binding parameters required for proper quantitative analysis of receptor-receptor interactions. Therefore,

TABLE 1

Binding parameters of M_1, M_2, and M_3 mAChR constructs

HEK 293 cells were transfected with *R*Luc-tagged, YFP-tagged, or nontagged (WT) mAChR, and [^{3}H]QNB saturation binding studies were performed as described under "Experimental Procedures." Curves were fitted by nonlinear regression analysis by assuming a single binding site, and K_d values were determined by using GraphPad Prism software. Results represent means ± S.E. ($n = 3$).

Construct	K_d
	*p*M
M_1 mAChR-*R*Luc	13.7 ± 0.9
M_1 mAChR-YFP	13.0 ± 0.7
WT-M_1 mAChR	11.7 ± 2.0
M_2 mAChR-*R*Luc	19.4 ± 2.0
M_2 mAChR-YFP	24.6 ± 3.3
WT-M_2 mAChR	24.0 ± 2.8
M_3 mAChR-*R*Luc	38.6 ± 3.2
M_3 mAChR-YFP	33.6 ± 4.2
WT-M_3 mAChR	37.8 ± 2.5

[4] J. C. Goin and N. M. Nathanson, unpublished observations.

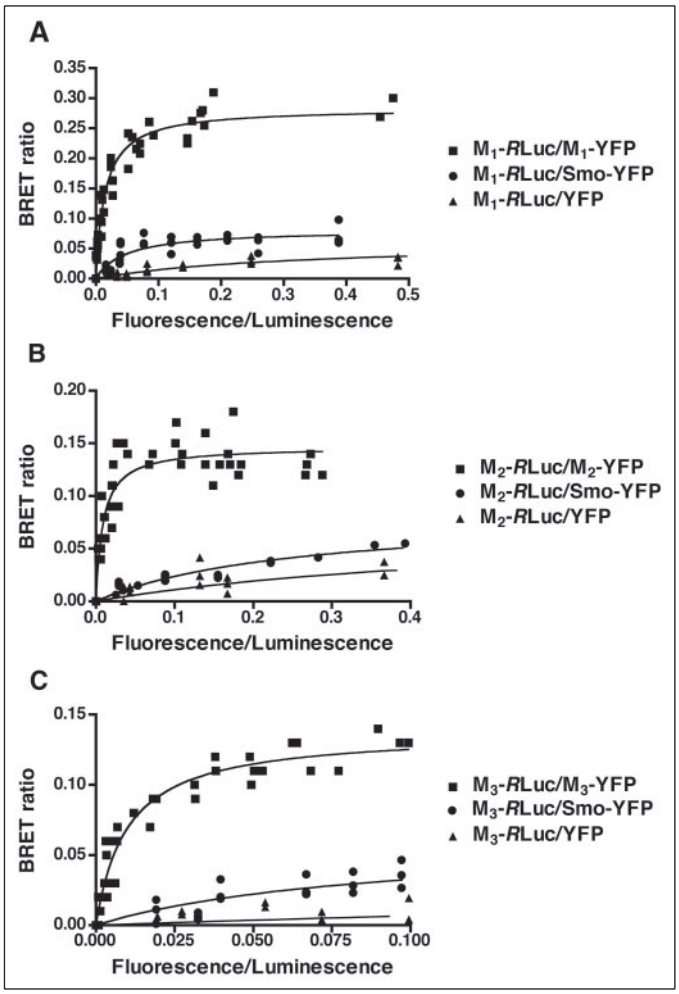

FIGURE 1. **Detection of constitutive M_1, M_2, and M_3 mAChR homodimers in live cells by BRET saturation assays.** HEK 293 cells were cotransfected with a constant DNA concentration of M_1-*R*Luc (*A*), M_2-*R*Luc (*B*), or M_3-*R*Luc (*C*) and increasing concentrations of the corresponding mAChR-YFP, Smo-YFP, or YFP constructs. BRET, total luminescence, and total fluorescence were determined 36 h after transfection. BRET ratio values were plotted as a function of the total fluorescence/total luminescence ratio. This ratio reflects the expression levels of the YFP construct that have been normalized by the expression levels of the *R*Luc construct to rule out the influence of any degree of variability in the levels of the *R*Luc fusion protein when this construct coexpressed different amounts of the YFP fusion protein. All values are expressed from data obtained in 3–7 independent experiments. The curves were fitted using a nonlinear regression equation assuming a single binding site (GraphPad Prism).

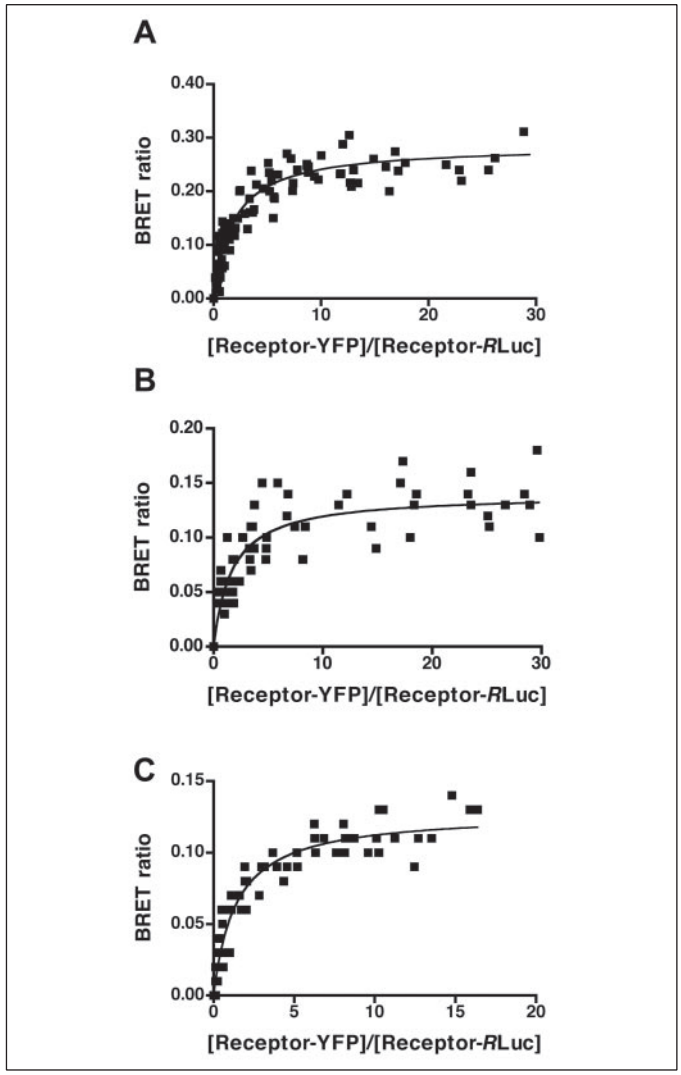

FIGURE 2. **Quantitative analysis of M_1, M_2, and M_3 homodimerization; BRET saturation curves.** BRET donor saturation curves of M_1, M_2, and M_3 mAChR homodimers were performed by transfecting HEK 293 cells with a constant DNA concentration of M_1-*R*Luc (*A*), M_2-*R*Luc (*B*), or M_3-*R*Luc (*C*) and increasing concentrations of M_1-YFP, M_2-YFP, or M_3-YFP constructs, respectively. BRET, total fluorescence, and total luminescence values were determined as described under "Experimental Procedures." Fluorescence and luminescence values were transformed into receptor numbers using slope values from standard titration curves shown in supplemental Fig. 2. BRET values were plotted as a function of the (receptor-YFP)/(receptor-*R*Luc) ratio. The total numbers of receptors expressed (fmol/mg protein) ranged as follows: (M_1-*R*Luc) + (M_1-YFP), 120–800; (M_2-*R*Luc) + (M_2-YFP), 210–1010; (M_3-*R*Luc) + (M_3-YFP), 240–1110. The curves represent 4–7 saturation curves that were fitted using a nonlinear regression equation assuming a single binding site (GraphPad Prism).

we conducted a new set of saturation experiments in which the amount of each receptor effectively expressed in transfected cells was monitored, for each individual experiment, by correlating both total luminescence and total fluorescence with the number of [^{3}H]QNB-binding sites. The analysis of such correlation shows a linear relationship between total luminescence and receptor density with no significant differences among the slopes obtained for the three mAChR receptor subtypes (supplemental Fig. 2). Correlation analysis between total fluorescence and total receptor numbers also yielded linear curves. However, the slope obtained for M_1-YFP was significantly higher than that from either M_2-YFP or M_3-YFP. The linear regression equations shown in supplemental Fig. 2 were used to transform fluorescence and luminescence units to receptor numbers, and BRET signals were plotted as a function of (receptor-YFP number)/(receptor-*R*Luc number) ratio. These new BRET saturation curves also behaved as hyperbolic functions reaching a saturation level (Fig. 2). According to classical analysis of BRET-monitored protein-protein interaction assuming one binding site, the concentration of the acceptor giving 50% of the energy transfer ($BRET_{50}$) accounts for the relative affinity between both interacting protomers, and the maximal BRET signal depends on the total number of dimers formed as well as on the distance between the donor and the acceptor within the dimer (19). When comparing the curves obtained for M_1, M_2, and M_3 mAChR homodimers (Table 2), no significant differences in $BRET_{50}$ values were found, indicating that the affinities of protomers for one another are similar among the three mAChR subtypes studied. On the other hand the $BRET_{max}$ value for the M_1 donor-acceptor pair was found to be significantly different from that for M_2 and M_3 homodimers. Indeed, the $BRET_{max}$ for the M_1-*R*Luc/M_1-YFP pair was over twice as high as the other $BRET_{max}$ values. This could indicate that either a higher percentage of the M_1 subtype is engaged in homodimerization or that energy transfer between *R*Luc and YFP within the M_1 homodimer is more efficient than that for M_2 and M_3 homodimers. Because the relative affinities between

TABLE 2

Homodimerization of M_1, M_2, and M_3 mAChR; parameters from BRET saturation curves

The $BRET_{max}$ is the maximal BRET ratio obtained for a given pair. The $BRET_{50}$ represents the acceptor/donor ratio required to reach half-maximal $BRET_{max}$ values. The percentage of homodimers was also estimated. By assuming a free equilibrium between the donor and acceptor construct for each receptor subtype, only 50% of the dimers can generate BRET if both constructs are expressed at equimolar levels. If 100% of the receptors exist as dimers, the expected BRET values would be $BRET_{max}/2$ (0.143, 0.070, and 0.064 for M_1, M_2, and M_3 homodimers, respectively). The average experimental BRET values of 0.126 (M_1), 0.052 (M_2), and 0.053 (M_3) obtained upon expression of equimolar amounts donor and acceptor fusion proteins at different expression levels of total receptors generate the % values indicated. Results are the mean ± S.E. of 4–7 experiments performed in duplicate.

Pair transfected	$BRET_{max}$	$BRET_{50}$	% of receptors existing as dimers
M_1-*R*Luc/M_1-YFP	0.285 ± 0.007	1.83 ± 0.14	72 ± 4
M_2-*R*Luc/M_2-YFP	0.139 ± 0.004	1.70 ± 0.23	78 ± 8
M_3-*R*Luc/M_3-YFP	0.128 ± 0.003	1.41 ± 0.13	83 ± 6

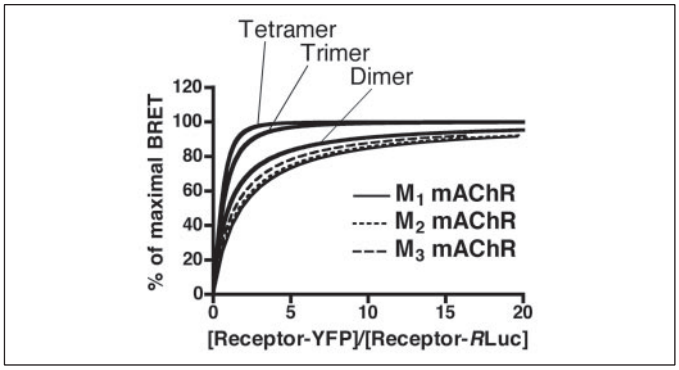

FIGURE 3. **Assessment of the nature of M_1, M_2, and M_3 mAChR homo-oligomers.** The experimental curves for M_1, M_2, and M_3 homo-oligomers shown in Fig. 2 were compared with the expected BRET saturation curves for dimeric, trimeric, and tetrameric complexes. These theoretical curves were calculated using an equation that determines the probability of forming BRET-competent complexes as a function of the size of the oligomer (19). BRET competent complexes = $((a + d)^n - a^n - d^n)/((a + d)^n - a^n - d^n + nd^n)$, where n is the number of receptor molecules in the complex; d is the number of receptor-*R*Luc (energy donor); a is the number of receptor-YFP (energy acceptor). Data on the y axis expressed as percent maximal BRET are plotted as a function of the (receptor-*R*Luc)/(receptor-YFP) ratio.

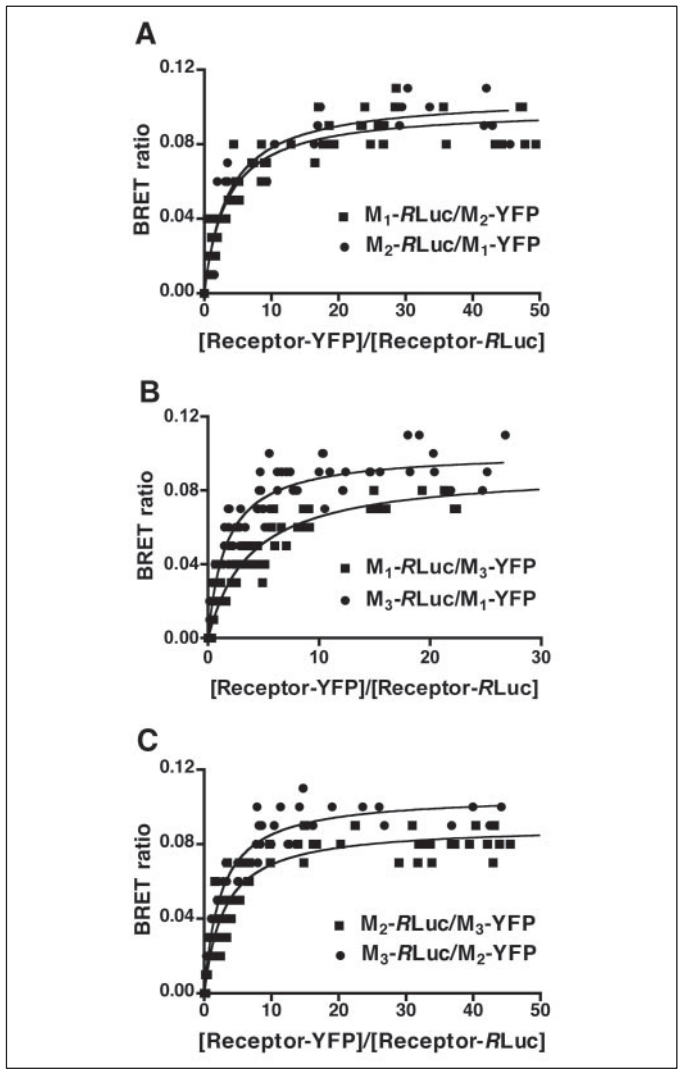

FIGURE 4. **Quantitative analysis of M_1, M_2, and M_3 heterodimerization.** BRET donor saturation curves of M_1/M_2 (*A*), M_1/M_3 (*B*), and M_2/M_3 (*C*) mAChR heterodimers were performed by transfecting HEK 293 cells with a constant DNA concentration of receptor-*R*Luc and increasing concentrations of receptor-YFP constructs for each pair at the two possible transfer orientations. BRET, total fluorescence, and total luminescence values were determined as described under "Experimental Procedures." Fluorescence and luminescence values were transformed into receptor numbers using slope values from standard titration curves shown in supplemental Fig. 2. BRET values were plotted as a function of the (receptor-YFP)/(receptor-*R*Luc) ratio. The total numbers of receptors expressed (fmol/mg protein) ranged as follows: (M_1-*R*Luc) + (M_2-YFP), 120–1030; (M_2-*R*Luc) + (M_1-YFP), 180–920; (M_1-*R*Luc) + (M_3-YFP), 170–680; (M_3-*R*Luc) + (M_1-YFP), 250–1290; (M_2-*R*Luc) + (M_3-YFP), 510–1150; (M_3-*R*Luc) + (M_2-YFP), 144–1020. The curves represent 4–6 saturation curves that were fitted using a nonlinear regression equation assuming a single binding site (GraphPad Prism).

each of the partners were found to be very similar among the three receptor subtypes (Table 2), the second hypothesis is more likely. Moreover, the fact that correlation curves between total fluorescence and receptor density yielded a higher slope value for M_1 suggests that YFP functions as a more efficient acceptor when it is fused to the M_1 receptor subtype, which may result in higher BRET values for this pair.

To assess the nature of M_1, M_2, and M_3 mAChR homo-oligomers, we compared their corresponding experimental saturation curves (Fig. 2) with the expected ones for dimeric, trimeric, and tetrameric complexes using a modification of the equation by Veatch and Stryer (24). This formula describes the probability of forming BRET-competent complexes as a function of the oligomeric size of the receptor (19). The experimental curves fit better to the theoretical curve predicted for a dimer rather than those expected for a trimer or tetramer, suggesting that the oligomeric fraction of M_1, M_2, or M_3 mAChR populations is predominantly composed of dimeric complexes (Fig. 3).

Detailed quantitative analysis of β_2-adrenergic receptor homodimerization by Mercier *et al.* (19) suggested that it is possible to estimate the proportion of receptors engaged in dimerization. Assuming a free equilibrium between donor and acceptor fusion proteins, only 50% of the dimers are expected to generate BRET if both partners are expressed at equimolar concentrations, because each partner can also generate 25% homodimers between identical molecules. Thus, if all receptors form dimers, the maximal BRET ratio detected at equimolar expression levels should be $BRET_{max}/2$. We determined experimental BRET values corresponding to equimolar expression of donor/acceptor at different expression levels of total receptors (Table 2, legend). Predicted percentage values of M_1, M_2, and M_3 mAChR existing as dimers are shown in Table 2 and suggest that a population of a single subtype of M_1, M_2, or M_3 mAChR is predominantly composed of constitutive homodimers.

Because different subtypes of endogenous mAChR are frequently coexpressed in various cell types, we also investigated whether M_1, M_2, and M_3 mAChR can interact with each other by forming heterodimers in live cells. To test this hypothesis, we cotransfected HEK 293 cells with all possible combinations of mAChR-*R*Luc and mAChR-YFP constructs and performed BRET saturation curve analysis as indicated previously. Again, curves were also best fit for one-binding site hyperbolas

TABLE 3

Heterodimerization of M_1, M_2, and M_3 mAChR; parameters from BRET saturation curves

The $BRET_{max}$ is the maximal BRET ratio obtained for a given pair. The $BRET_{50}$ represents the acceptor/donor ratio required to reach half-maximal BRET values. Results are the mean ± S.E. of 4–6 experiments performed in duplicate.

Pair transfected	$BRET_{max}$	$BRET_{50}$
M_1-*R*Luc/M_2-YFP	0.099 ± 0.002	3.37 ± 0.31
M_2-*R*Luc/M_1-YFP	0.106 ± 0.005	3.56 ± 0.56
M_1-*R*Luc/M_3-YFP	0.091 ± 0.002	3.81 ± 0.30
M_3-*R*Luc/M_1-YFP	0.101 ± 0.002	1.65 ± 0.14[a]
M_2-*R*Luc/M_3-YFP	0.090 ± 0.002	3.01 ± 0.27
M_3-*R*Luc/M_2-YFP	0.106 ± 0.002	2.49 ± 0.19

[a] This is significantly different from its reverse combination ($p < 0.001$).

by nonlinear regression analysis indicating that mAChR can also heterodimerize in intact cells (Fig. 4). Comparisons between $BRET_{50}$ values obtained from those curves (Table 3) showed no significant differences between M_1-*R*Luc/M_2-YFP or M_2-*R*Luc/M_3-YFP and their reverse orientations. However, M_3-*R*Luc/M_1-YFP exhibited a significantly lower $BRET_{50}$ value than its reverse combination ($p < 0.001$). Although such a difference is small enough and both $BRET_{50}$ values are still consistent with the presence of high affinity heterodimers, it suggests that the relative position of the donor and the acceptor moieties could somewhat interfere with receptor-receptor interaction. Actually, the BRET technology used in this work has been shown to be sensitive enough to detect conformational changes depending on the donor-acceptor combination within a given heterodimeric pair. When assessing the effects of ligands on the BRET signal observed for the MT1/MT2 melatonin receptor heterodimer, Ayoub *et al.* (25) obtained drastically different results for the two possible orientations; although BRET from MT2R-*R*Luc to MT1R-YFP was ligand-insensitive, all ligands tested increased BRET for the reverse orientation. The recently introduced $BRET^2$ methodology (19), which allows a better separation between the donor and the acceptor emission spectra, could be a useful alternative to examine the discrepancy between $BRET_{50}$ values for the two M_1/M_3 combinations obtained by the BRET approach. Regardless of the $BRET_{50}$ value for this construct, most combinations resulted in slightly but consistently higher $BRET_{50}$ values than those from homodimers sharing either tagged partner. $BRET_{max}$ values for all possible combinations of heterodimers, which ranged from 0.09 to 0.11, were found to be significantly lower than those found for all homodimers ($p < 0.05$) (Table 3). As discussed above, this could mean either that the total number of mAChR heterodimers is lower than the total number of homodimers at the same experimental conditions or that the relative position of *R*Luc and YFP within heterodimers is less permissive for energy transfer. Because relative affinity values within mAChR heterodimers are slightly but significantly lower than those for homodimers, we could infer that even though all mAChR subtypes can form heterodimers in intact cells, the likelihood of homodimer formation appears to be slightly but consistently higher compared with that for heterodimers. However, we cannot rule out the effect of the relative position of the donor and acceptor moieties on the efficiency of energy transfer, which is also reflected in $BRET_{max}$ values. Taken together, these results suggest that heterogeneous populations of M_1/M_2, M_1/M_3, or M_2/M_3 exist as a combination of high affinity homo- and heterodimers, most probably with a minor proportion of monomers. The exact composition of a heterogeneous combination of M_1, M_2, and/or M_3 mAChR would depend on both the amount of each mAChR partner and also on the relative affinity between them.

Two observations suggested that we can rule out the possibility that BRET signals obtained in the BRET saturation curves resulted from receptor construct overexpression. First, the expression levels of total receptors in our BRET saturation experiments are comparable with those observed in native tissues. Indeed, the lowest level of total receptor expression that allowed detection of BRET in our studies ranged from 12 to 510 fmol/mg protein (see Figs. 2 and 4 legends). These total mAChR expression levels are comparable with or lower than those found in mouse thalamus (355 fmol/mg protein) and hypothalamus (337 fmol/mg protein) (26), canine right atrium (947–1455 fmol/mg protein) (27), and mouse striatum (1185 fmol/mg protein) (26). Second, we observed that equimolar expression of receptor-*R*Luc and receptor-YFP proteins in different experiments resulted in similar BRET values, regardless of the total receptor expression levels.[4] If such BRET values had resulted from a spurious interaction between receptor-*R*Luc and receptor-YFP fusion proteins, we would have expected a proportional increase in BRET signals as the total level of receptor expression increased.

TABLE 4

Effect of agonist treatment on of M_1, M_2, and M_3 mAChR homodimerization; parameters from BRET saturation curves

HEK 293 cells were transfected with a constant DNA concentration of M_1-*R*Luc, M_2-*R*Luc, or M_3-*R*Luc and increasing concentrations of M_1-YFP, M_2-YFP, or M_3-YFP constructs, respectively. After a 36-h incubation period, cells were treated with 10 μM carbachol at 25 °C for different times, and BRET, total fluorescence, and total luminescence values were determined as described under "Experimental Procedures." BRET ratio levels were expressed as a function of the [acceptor]/[donor] ratio using the experimental titration curves shown in supplemental Fig. 2, and curves were fitted using a nonlinear regression equation assuming a single binding site (GraphPad Prism). $BRET_{max}$ and $BRET_{50}$ values are presented as the mean ± S.E. ($n = 3$). Similar results were obtained by incubating transfected cells with 10 μM carbachol at 37 °C or 100 μM carbachol at 25 °C.[4]

Pair transfected	Time	$BRET_{max}$	$BRET_{50}$
	min		
M_1-*R*Luc/M_1-YFP	0	0.231 ± 0.008	1.31 ± 0.19
	5	0.252 ± 0.009	1.44 ± 0.20
	15	0.231 ± 0.008	1.41 ± 0.13
	30	0.237 ± 0.008	1.10 ± 0.15
M_2-*R*Luc/M_2-YFP	0	0.130 ± 0.008	1.39 ± 0.33
	5	0.134 ± 0.011	1.80 ± 0.58
	15	0.128 ± 0.007	1.48 ± 0.30
	30	0.154 ± 0.009	1.55 ± 0.38
M_3-*R*Luc/M_3-YFP	0	0.167 ± 0.006	1.36 ± 0.24
	5	0.170 ± 0.006	1.32 ± 0.24
	15	0.171 ± 0.006	1.62 ± 0.29
	30	0.158 ± 0.005	1.01 ± 0.17

Evidence that agonists can induce changes in BRET signal has been reported for several GPCR. Eventually, such changes in energy transfer either reflect variations in dimer formation or just conformational changes within pre-existing dimers (2). In contrast, other studies have failed to show BRET changes upon agonist treatment (3). Therefore, we investigated the effect of a muscarinic agonist on BRET by performing BRET saturation curves on HEK 293 cells cotransfected with all possible combinations of M_1, M_2, and M_3 donor and acceptor fusion proteins. Carbachol (10 μM) treatment during 5, 15, or 30 min of transfected cells revealed no significant changes in BRET signal for any of the receptor pairs tested (Tables 4 and 5 and see supplemental Figs. 3 and 4). These results suggest that agonist treatment does not modify homo- or heterodimer formation or even promote permanent conformational changes that could modify BRET within pre-existing dimers.

To determine the functional implications of mAChR oligomerization, we investigated whether mAChR heterodimerization can induce changes in agonist-promoted receptor down-regulation. Previous work has shown that different mAChR subtypes exhibit different sensitivities to agonist-induced down-regulation when expressed in JEG-3 cells (21). Our first goal was to determine whether M_2 and M_3 mAChR individually expressed on JEG-3 cells exhibited a differential down-regulation pattern upon sustained agonist stimulation. mAChR down-regulation

TABLE 5

Effect of agonist treatment on of M_1, M_2, and M_3 mAChR heterodimerization; parameters from BRET saturation curves

BRET donor saturation curves of M_1/M_2, M_1/M_3, and M_2/M_3 mAChR heterodimers were performed by transfecting HEK 293 cells with a constant DNA concentration of receptor-*R*Luc and increasing concentrations of receptor-YFP constructs for each pair at the two possible transfer orientations. BRET, total fluorescence, and total luminescence values were determined as described under "Experimental Procedures." After a 36-h incubation period, cells were treated with 10 μM carbachol at 25 °C for different times, and BRET, total fluorescence and total luminescence values were determined as described under "Experimental Procedures." Fluorescence and luminescence values were transformed into receptor numbers using slope values from standard titration curves shown in supplemental Fig. 2, and curves were fitted using a nonlinear regression equation assuming a single binding site (GraphPad Prism). $BRET_{max}$ and $BRET_{50}$ values are presented as the mean ± S.E. ($n = 3$).

Pair transfected	Time	$BRET_{max}$	$BRET_{50}$
	min		
M_1-*R*Luc/M_2-YFP	0	0.106 ± 0.004	3.46 ± 0.81
	5	0.108 ± 0.004	6.77 ± 1.34
	15	0.108 ± 0.004	6.57 ± 0.16
	30	0.108 ± 0.005	5.72 ± 1.13
M_2-*R*Luc/M_3-YFP	0	0.171 ± 0.007	3.10 ± 0.50
	5	0.165 ± 0.006	3.01 ± 0.45
	15	0.164 ± 0.006	3.27 ± 0.48
	30	0.168 ± 0.004	3.16 ± 0.29
M_3-*R*Luc/M_1-YFP	0	0.168 ± 0.010	1.67 ± 0.46
	5	0.161 ± 0.011	1.68 ± 0.44
	15	0.152 ± 0.010	1.59 ± 0.43
	30	0.157 ± 0.008	1.61 ± 0.35
M_1-*R*Luc/M_3-YFP	0	0.165 ± 0.007	3.90 ± 0.63
	5	0.159 ± 0.006	3.89 ± 0.59
	15	0.152 ± 0.006	3.81 ± 0.69
	30	0.159 ± 0.003	3.88 ± 0.36
M_2-*R*Luc/M_1-YFP	0	0.154 ± 0.007	3.52 ± 0.57
	5	0.154 ± 0.005	3.92 ± 0.56
	15	0.152 ± 0.006	4.08 ± 0.73
	30	0.159 ± 0.003	4.16 ± 0.38
M_3-*R*Luc/M_2-YFP	0	0.154 ± 0.007	2.46 ± 0.40
	5	0.149 ± 0.005	2.54 ± 0.31
	15	0.152 ± 0.006	2.85 ± 0.52
	30	0.159 ± 0.003	2.91 ± 0.27

was determined as the decrease in total cellular muscarinic binding sites using the lipophilic muscarinic antagonist [^{3}H]QNB. Carbachol treatment (1 mM) of JEG-3 cells transfected with M_2 mAChR resulted in a time-dependent decrease in the total number of mAChR-binding sites, reaching its maximum 73 ± 3% decrease in receptor number at 12 h, as compared with control transfected, untreated cells (Fig. 5*A*). In contrast, carbachol treatment of cells expressing FLAG-M_3 mAChR promoted a substantially lower maximal extent of receptor down-regulation, compared with the decrease in M_2 (M_3, 36 ± 4%, $p < 0.01$). The kinetic analysis revealed a first rate process with similar rate constants for receptor subtypes ($t_{1/2}$ (h) M_2, 2.4 ± 0.1; M_3, 2.5 ± 0.2) (Fig. 5*A*, *inset*). Carbachol-induced differential down-regulation of M_2 and M_3 mAChR was confirmed by concentration-response curves, which again showed significantly different maximal effects (E_{max} (%) M_2, 65 ± 4; M_3, 24 ± 3, $p < 0.02$) but similar EC_{50} values for both receptor subtypes (EC_{50} (μM) M_2, 2.2 ± 0.1; M_3, 1.8 ± 0.2) (Fig. 5*B*).

Given that both M_2 and M_3 mAChR are coexpressed in many tissues, including the gastrointestinal tract, uterus, urinary bladder, ciliary body, and airways (28) and that they were also found to form heterodimers (Fig. 3), we asked whether M_2/M_3 heterodimerization could modify the differential pattern of M_2/M_3 receptor regulation in JEG-3 cells coexpressing both receptor subtypes. Thus, we treated cells expressing M_2 mAChR alone, FLAG-tagged M_3 mAChR alone, or both receptors at different proportions with 10 μM carbachol for 12 h and determined the extent of subtype-specific receptor down-regulation by immunoprecipitation of solubilized [^{3}H]QNB-labeled M_2 or FLAG-M_3 mAChR using anti-M_2 or anti-FLAG monoclonal antibodies, respectively. Agonist stimulation of cells expressing M_2 mAChR alone resulted in a 43.4 ± 5.4% decrease in cellular receptor numbers, whereas treatment of cells expressing only FLAG-M_3 mAChR led to a 15.0 ± 4.6% loss of [^{3}H]QNB-binding sites, as assessed by immunoprecipitation, which was consistent with the binding assay results described above (Fig. 6). Most strikingly, coexpression of JEG-3 cells with FLAG-M_3 mAChR and increasing proportions of M_2 mAChR led to a concentration-dependent increase in FLAG-M_3 mAChR down-regulation, with a maximal 43.5 ± 3.3% decrease in receptor number, as compared with control untreated cells. In contrast, the extent of M_2 mAChR down-regulation remained unchanged within the same range of receptor ratio values.[4]

To rule out the possibility that the coexpression of the M_2 receptor increases the FLAG-M_3 receptor down-regulation because of an unanticipated effect of the FLAG tag, we performed control experiments by cotransfecting the FLAG-tagged M_3 mAChR in the presence of increasing amounts of a non-FLAG-tagged M_3 mAChR (HA-M_3). In this case, the extent of FLAG M_3 down-regulation was not significantly altered at any HA-M_3/FLAG-M_3 expression ratio tested (Fig. 6).

Taken together, these data indicate that coexpression of M_2 and M_3 mAChR facilitates M_3 receptor regulation by forming M_2/M_3 heterodimers that are more susceptible of being regulated by agonist exposure than M_3 alone.

DISCUSSION

Evidence supporting the ability of mAChR to form dimers or higher order oligomers has been provided by a wide variety of approaches spanning basic pharmacological analysis of ligand-receptor interactions to biochemical assessment of protein-protein interactions by coimmunoprecipitation and immunoblotting assays (29). However, the direct interaction between partners involved in mAChR homo- and heterodimerization in their physiological environment has not yet been characterized.

Resonance energy transfer approaches (fluorescence resonance energy transfer and BRET) have become systems of choice to monitor protein-protein interactions in living cells (2). Because BRET between *R*Luc and YFP can occur only if both molecules are within ~100 Å of each other, the occurrence of BRET between *R*Luc- and YFP-tagged fusion proteins indicates a molecular proximity that is consistent with dimerization (12). In this study we use the term dimer as the simplest form of oligomerization, and we eventually discuss the possibility that BRET could also result from the existence of larger complexes.

Our results from BRET saturation analysis show that M_1, M_2, and M_3 can form homo-oligomers in intact HEK 293 cells. Indeed, the interaction between mAChR-*R*Luc and mAChR-YFP partners within each oligomer studied has proved to be saturable and specific. The specificity of mAChR oligomerization was demonstrated by BRET saturation curves showing the inability of M_1, M_2, and M_3 receptors to heterodimerize with an unrelated seven transmembrane domain protein, the signaling receptor Smoothened (Smo). The potential inability of Smo-YFP to engage in oligomerization was ruled out by the demonstration that this fusion protein interacts with Smo-*R*Luc to yield a saturable BRET signal consistent with Smo homodimerization (supplemental Fig. 1), as was suggested previously (30). Further evidence supporting the specificity of mAChR oligomerization is derived from a β-galactosidase complementation approach by Kaykas *et al.* (15) who have recently demonstrated that the unrelated GPCR Frizzled 1 and Frizzled 2 can homodimerize and even heterodimerize with each other, but not with M_1 or M_2 mAChR. More recently, it has been reported that μ, δ, or κ opioid receptors do not form detectable hetero-oligomers with M_2 mAChR by using the BRET^2 technology (31).

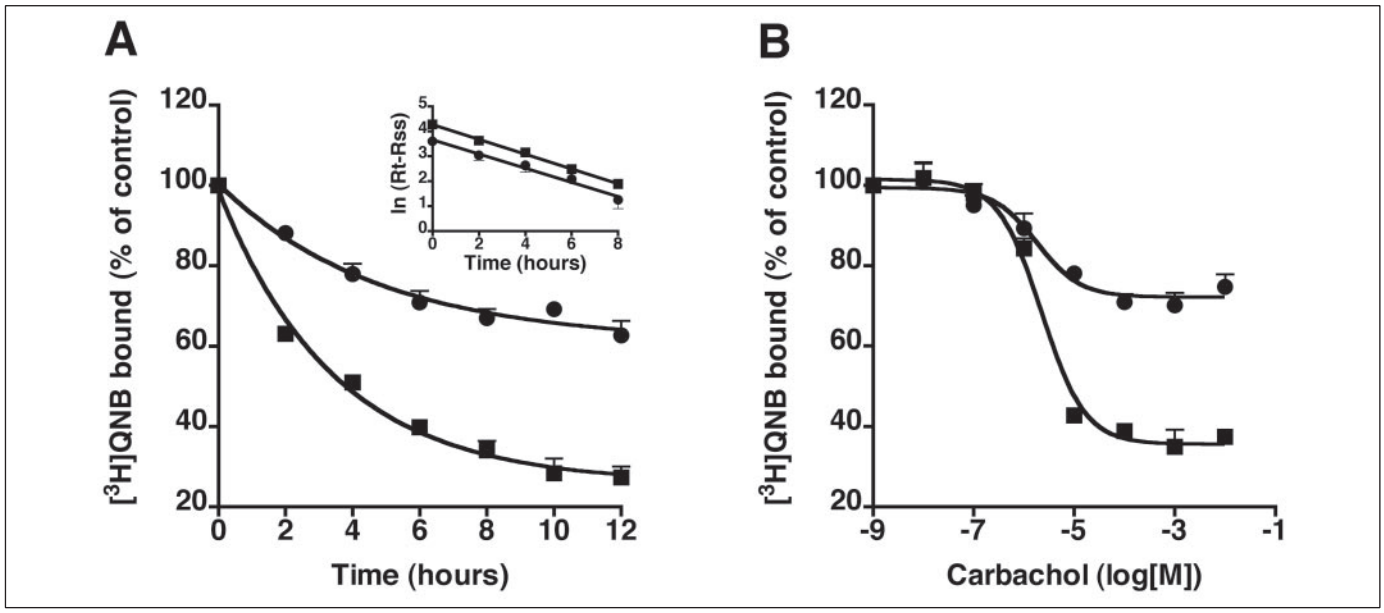

FIGURE 5. **Differential agonist-induced down-regulation of M_2 and M_3 mAChR.** JEG-3 cells were transiently transfected with either nontagged M_2 or FLAG-tagged M_3 mAChR and treated or not with either 1 mM carbachol for various incubation times (*A*) or various concentrations of carbachol for 12 h (*B*) at 37 °C. Total receptors were measured in whole cells using the membrane-permeable muscarinic antagonist [^{3}H]QNB as described under "Experimental Procedures." Data are expressed as the percent of receptors down-regulated and represent the means ± S.E. of four independent experiments performed in triplicate. *A,* the data shown in the main figure are fit to first-order exponential decay curves using GraphPad Prism, and the *inset* shows the kinetic analysis of the rate of mAChR number loss after carbachol treatment. *Rt* indicates the receptor number at the indicated time after carbachol exposure. *Rss* indicates the steady state receptor number at 12 h after carbachol treatment. *B,* data were fit as a sigmoid function using GraphPad Prism. *Squares*, M_2 mAChR; *circles,* FLAG-M_3 mAChR.

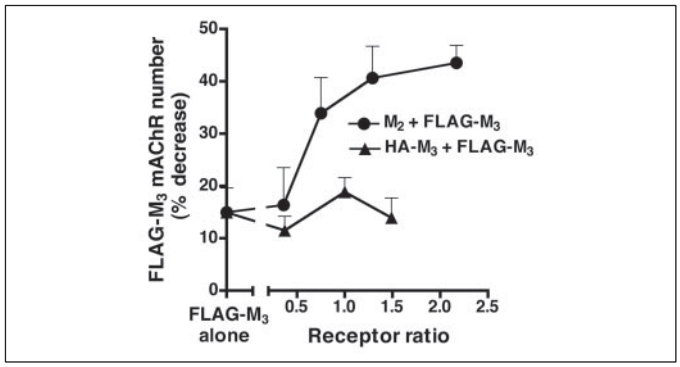

FIGURE 6. **Effect of M_2/M_3 mAChR heterodimerization on M_3 mAChR down-regulation.** JEG-3 cells were transfected with FLAG-tagged M_3 mAChR in the presence or absence of increasing amounts of either M_2 mAChR (*circles*) or HA-M_3 mAChR (*triangles*). The cells were then treated with 10 μM carbachol for 12 h, and the extent of FLAG-M_3 mAChR down-regulation was determined by immunoprecipitation of solubilized [^{3}H]QNB labeled with anti-FLAG monoclonal antibodies, as described under "Experimental Procedures." Results are expressed as the percentage decrease in FLAG-M_3 receptor number as compared with control transfected, untreated cells and represent the means ± S.E. of 3–8 independent experiments performed in duplicate. Receptor ratio, M_2/FLAG-M_3 (*circles*) and HA-M_3/FLAG-M_3 (*triangles*).

The existence of constitutive M_1, M_2, and M_3 mAChR homodimers in live cells shown here correlates with previous pharmacological and biochemical data already discussed in the Introduction and provides further characterization of the interaction between protomers within the oligomeric complexes. In fact, the analysis of $BRET_{50}$ values from BRET saturation curves, which reflects the relative affinity of the receptor partners for one another, suggests that the three receptor subtypes have a similar propensity to homodimerize (Table 2). Our data also suggest that the majority of M_1, M_2, or M_3 mAChR individually expressed in HEK 293 cells are engaged in BRET-competent complexes and that the "dimer" is the predominant form within the oligomeric population. These results are supported by other studies using BRET and cell surface biotinylation assays, which demonstrated that most if not all β_2-adrenergic, opioid, melatonin, and adenosine A_{2A} receptors exist as dimeric complexes in the plasma membrane (19, 25, 31, 32). In contrast, our data present a different view from previous biochemical reports suggesting the existence of M_1, M_2, and M_3 mAChR higher order homo-oligomers (9, 33). In particular, the recent work by Park and Wells (34) has suggested the existence of trimeric or even larger aggregates in extracts from solubilized M_2 mAChR expressed in *Sf*9 cells. Because of the highly hydrophobic nature of mAChR TMD and the extreme levels of protein expression reached in *Sf*9 cells, it could be argued that detection of oligomers by this methodology results from artifactual aggregation following cell lysis and solubilization (10). The results shown in this report using the BRET methodology suggest that M_1, M_2, and M_3 mAChR expressed in live cells are populations composed of a predominant fraction of homodimers and a minor fraction of monomers. However, we cannot rule out the existence of higher order complexes that cannot be detected by BRET because of distance constraints.

Although most previous reports in favor of the existence of mAChR oligomers have agreed that these GPCR can form homodimers, the existence of constitutive mAChR heterodimers remains controversial. By using trans-complementation experiments, Maggio *et al.* (35) provided pharmacological evidence for the formation of M_2/M_3 heterodimers. Upon coexpression of wild type M_2 or M_3 mAChR with gene fragments originating from M_3 or M_2 mAChR, respectively, these authors determined the presence of two populations of binding sites as follows: one representing the wild type M_2 or M_3 receptors, and the other identified as a heterodimeric M_2/M_3 receptor. Recently, Novi *et al.* (36) reported that M_2 and M_3 receptors can interact physically by showing that HA-tagged M_3 mAChR could be immunoprecipitated with anti-Myc antibodies, and Myc-M_2 mAChR were immunoprecipitated with anti-HA antibodies when both receptors were coexpressed in COS-7 cells. These data have been challenged by other reports, which failed to provide evidence for the existence of mAChR heterodimers. For instance, Griffin *et al.* (37) compared the pharmacological antago-

nism of M_2 and M_3 mAChR expressed in Chinese hamster ovary cells both in isolation or in combination, and their binding and signaling data were consistent with those expected for independent receptors and not heteromeric complexes or the exhibition of a novel pharmacology. Moreover, biochemical evidence against M_3/M_1 and M_3/M_2 mAChR heterodimerization was provided by Zeng and Wess (9), who reported no detectable coimmunoprecipitation of an HA epitope-tagged M_3 mAChR with M_1 or M_2 mAChR in lysates from COS-7 cells cotransfected with either receptor pair. It is tempting to speculate that the biochemical approach that failed to show evidence for the existence of M_3/M_1 and M_3/M_2 heterodimers (9) was carried out using mutant M_3 receptors lacking most of the i3 loop, which might hamper the interaction with wild type M_1 or M_2 mAChR. In fact, trans-complementation assays by Maggio *et al.* (35) have shown that removal of a large fragment of the i3 loop from M_3 can prevent the interaction between this mutant receptor and a truncated form of M_2, and that such interaction can be rescued by using the wild type M_3 receptor instead of the short M_3 form. These data also appear to be consistent with the hypothesis proposed by Gouldson *et al.* (38), who suggested that GPCR dimers are generated by swapping TMD and proposes the integrity of the i3 loop as a requirement for receptor dimerization. However, biochemical data showing that the shortening of the i3 from M_3 did not prevent M_3 homodimerization (9) suggest that the presence of the full-length i3 loop is not required for the formation of M_3 receptor homodimers.

In this study we attempted to resolve the discrepancy between pharmacological and biochemical data by using quantitative BRET analysis of receptor-receptor interaction to determine whether mAChR can form heterodimers in living cells. In our BRET assays the wild type sequence of receptors is conserved. In addition, receptor constructs are expressed within a preserved cellular environment and at their proper location at the cell surface. Our results from BRET saturation curves clearly indicate that M_1, M_2, and M_3 can form heterodimers. $BRET_{50}$ values from M_1, M_2, and M_3 mAChR heterodimerization curves (Table 3), although significantly higher than those determined for mAChR homodimers (Table 2), are also indicative of high affinity heterodimers. In fact, similar high affinity values have been reported for other GPCR homo- or hetero-oligomers (18, 19, 39, 40). Therefore, our data suggest that the coexpression of two mAChR subtypes in a given tissue results in a heterogeneous combination of homo- and heterodimers, whose proportions depend on both the relative affinity between interacting species and their expression levels, and a minor complement of monomers.

Agonist binding to some GPCR induces or stabilizes the dimerized state, which is the form of the receptor that productively interacts with G proteins. Other GPCR exist as constitutive dimers, which are already formed in the endoplasmic reticulum, and some of them even undergo monomerization upon agonist stimulation (1–3). There are, however, divergent results for a number of GPCR depending on the method used to assess dimerization (3). By using SDS-PAGE and Western blot analysis of membrane extracts from COS-7 cells expressing a mutant M_3 mAChR, Zeng and Wess (9) showed that agonist-induced receptor stimulation had no significant effect on M_3 mAChR dimerization. Our results were consistent with such findings, because carbachol treatment of HEK 293 cells expressing homologous or heterologous combinations of M_1, M_2, and M_3 mAChR fusion proteins revealed no significant changes in the BRET signal, as compared with control untreated cotransfected cells. BRET saturation curve analysis has shown that M_1, M_2, or M_3 mAChR may exist as homogeneous populations predominantly composed of high affinity homodimers. Alternatively, a heterogeneous population of two mAChR subtypes exists as a combination of constitutive homo- and heterodimers, with a minimal proportion of monomers. Therefore, we can conclude that the absence of a significant change in the BRET signal following agonist stimulation indicates that muscarinic agonists do not induce monomerization/disaggregation of oligomers or even conformational changes that may modify the stability of the oligomeric complexes. However, we cannot rule out the possibility that agonist stimulation induces assembly/disassembly events without affecting the steady state proportion of mAChR receptors engaged in homo-/heterodimers.

The functional consequences of mAChR homo- and heterodimerization have not been extensively addressed. Novi *et al.* (41) have recently demonstrated that the paired activation of the two components of M_3 mAChR homodimer is required for induction of extracellular signal-regulated kinase 1/2 phosphorylation, whereas single activation of part of a heterodimer is sufficient for G protein activation. In addition, these authors reported that the recruitment of β-arrestin-1 by homodimeric M_3/M_3 and heterodimeric M_2/M_3 mAChR requires the paired activation of the single receptor components within the dimer (36, 41).

Although these results contribute to the understanding of the role of oligomerization on β-arrestin-mediated signaling, the functional implications of mAChR heterodimerization on receptor regulation have not yet been investigated. The M_2/M_3 heterodimer pair is particularly interesting to analyze for several reasons. (*a*) Coexpressed M_2 and M_3 mAChR subtypes mediate autonomic regulation of smooth muscle contraction in many tissues. (*b*) Some studies have argued against the existence of mAChR heterodimers. In particular, the presence of M_2/M_3 constitutive heterodimers has been challenged by recent reports and is still a matter of controversy (9, 35–37). (*c*) M_2 and M_3 mAChR regulation has typically been examined using cell systems expressing a single mAChR subtype. This model differs from the physiological situation, in which different mAChR subtypes coexist, even together with less or nonrelated receptors.

Much has been learned about short term desensitization (G protein uncoupling, internalization/sequestration), which regulates GPCR within seconds to minutes after agonist-induced activation. Considerably less is known about biochemical mechanisms that regulate GPCR activity upon sustained agonist exposure. Long term regulation of GPCR, or "down-regulation," is thought to be important to physiological adaptation induced by endogenous ligands as well as to the clinical effects of exogenously administered drugs that are used in a chronic or repeated manner. Moreover, mutational analyses of mAChR and other GPCR have demonstrated that short term and long term receptor regulation pathways can be differentiated. In particular, we have shown previously that the long term down-regulation and the rapid sequestration of M_1 and M_2 mAChR are independent processes involving distinct molecular mechanisms (42, 43). Tsuga *et al.* (44) have also investigated differential regulatory mechanisms of M_2 mAChR upon agonist stimulation and demonstrated that internalization depends on the integrity of i3 (which becomes phosphorylated by GRK2 (G protein-coupled receptor kinase 2)), although down-regulation may occur through a GRK2 facilitating pathway and i3 independent pathway. The differential "short" *versus* "long" term regulation may be critical when choosing a cell system to assess mAChR regulation. In fact, M_1 and M_2 mAChR expressed in HEK 293 cells undergo agonist-induced internalization but not down-regulation (45, 46).

JEG-3 choriocarcinoma cells have proved to be a validated model to study the differential regulation of muscarinic receptor subtypes (14, 21, 43, 47). When M_1 or M_2 mAChR are expressed in these cells, sustained agonist stimulation leads to consistently higher levels of receptor down-regulation for M_2 than for M_1. Schlador *et al.* (21) identified five amino acids ("VTILA") located in TMD6, TMD7, and i3 that are essential for

M_2 mAChR regulation via a dynamin-independent mechanism. These residues are not present in M_1 mAChR, but substitution of this motif into the M_1 mAChR is sufficient for conversion to the down-regulation-competent M_2 phenotype.

Because the M_3 mAChR subtype also lacks the VTILA motif, we suspected that this receptor would show an impaired receptor regulation profile compared with M_2. Consistent with our predictions, M_2 underwent agonist-induced down-regulation to a much higher extent than M_3. Because we demonstrated previously that most of the M_2 and M_3 mAChR exist as constitutive homodimers (Figs. 1 and 2) and that agonist exposure does not induce changes in M_2 and M_3 homodimerization (Table 4), these results indicate that a significant fraction of the M_2 homodimer undergoes down-regulation, whereas most, if not all, of the M_3 homodimer remains at the cell surface.

Our previous results also suggest that a heterogeneous population of both M_2 and M_3 mAChR is composed of M_2 and M_3 homodimers together with a significant fraction of M_2/M_3 heterodimers, whose proportion depends on the expression levels of both receptor subtypes and the relative affinity values for both homodimers and the M_2/M_3 heterodimer. If such a heterogeneous population of receptors undergoes sustained agonist exposure, we would predict that M_2 and M_3 homodimers undergo differential down-regulation. To determine the fate of M_2/M_3 heterodimers, we first transfected JEG-3 cells with various proportions of M_2/FLAG-M_3, then subjected those cells to long term carbachol exposure, and finally determined the levels of total, M_2, and M_3 mAChR down-regulation using a subtype-specific mAChR immunoprecipitation protocol described previously (17). We observed that the extent of M_3 mAChR down-regulation increased as the M_2/M_3 expression level ratio was raised. Because the formation of M_2/M_3 heterodimers is promoted by gradually increasing the expression levels of M_2 (relative to M_3) (Fig. 4), and carbachol does not modify M_2/M_3 heterodimerization (Table 5), our results suggest that the increase in M_3 mAChR down-regulation is facilitated by the formation of M_2/M_3 heterodimers.

The mechanism by which M_2/M_3 heterodimers down-regulate more quickly than M_3 homodimers remains to be elucidated. However, we can speculate that the VTILA residues, which are essential for M_2 mAChR internalization and down-regulation in JEG-3 cells, may be involved in M_2/M_3 heterodimer internalization and down-regulation. According to this hypothesis, the endocytic machinery could recognize the VTILA motif present in the M_2 component and drive the whole M_2-M_3 complex into the endocytic pathway.

In summary, we have demonstrated that M_1, M_2, and M_3 mAChR form high affinity homo- and heterodimers in living cells and that the stability of those oligomers is not changed by short term agonist stimulation. In addition, our data suggest that agonist-induced M_3 mAChR down-regulation is enhanced as a result of M_2/M_3 heterodimerization, and our data support the notion that heterodimerization has potential implications on GPCR long term regulation.

Acknowledgments—We thank Stéphane Angers, Travis Biechele, and Ajamete Kaykas for providing reagents and for helpful discussions and assistance.

REFERENCES

1. Bouvier, M. (2001) *Nat. Rev. Neurosci.* **2,** 274–286
2. Angers, S., Salahpour A., and Bouvier, M. (2002) *Annu. Rev. Pharmacol. Toxicol.* **42,** 409–435
3. Breitwieser, G. E. (2004) *Circ. Res.* **94,** 17–27
4. Hirschberg, B. T., and Schimerlik, M. I. (1994) *J. Biol. Chem.* **269,** 26127–26135
5. Potter, L. T., Ballesteros, L. A., Bichajian, L. H., Ferrendelli, C. A., Fisher, A., Hanchett, H. E., and Zhang, R. (1991) *Mol. Pharmacol.* **39,** 211–221
6. Chidiac, P., and Wells, J. W. (1992) *Biochemistry* **31,** 10908–10921
7. Chidiac, P., Green, M. A., Pawagi, A. B., and Wells, J. W. (1997) *Biochemistry* **36,** 7361–7379
8. Maggio, R., Vogel, Z., and Wess, J. (1993) *Proc. Natl. Acad. Sci. U. S. A.* **90,** 3103–3107
9. Zeng, F. Y., and Wess, J. (1999) *J. Biol. Chem.* **274,** 19487–19497
10. Kroeger, K. M., Pfleger, K. D. G., and Eidne, K. A. (2004) *Front. Neuroendocrinol.* **24,** 254–278
11. Angers, S., Salahpour, A., Joly, E., Hilairet, S., Chelsky, D., Dennis, M., and Bouvier, M. (2000) *Proc. Natl. Acad. Sci. U. S. A.* **97,** 3684–3689
12. Xu, Y., Piston, D. W., and Johnson, C. H. (1999) *Proc. Natl. Acad. Sci. U. S. A.* **96,** 151–156
13. Luetje, C. W., Brumwell, C., Norman, M. G., Peterson, G. L., Schimerlik, M. I., and Nathanson, N. M. (1987) *Biochemistry* **26,** 6892–6896
14. Nadler, L. S., Kumar, G., and Nathanson, N. M. (2001) *J. Biol. Chem.* **276,** 10539–10547
15. Kaykas, A., Yang-Snyder, J., Héroux, M., Shah, K. V., Bouvier, M., and Moon, R. T. (2004) *Nat. Cell Biol.* **6,** 52–58
16. Mellon, P., Parker, V., Gluzman, Y., and Maniatis, T. (1981) *Cell* **27,** 279–288
17. Goin, J. C., and Nathanson, N. M. (2002) *J. Neurochem.* **83,** 964–972
18. Ayoub, M. A., Levoye, A., Delagrange, P., and Jockers, R. (2004) *Mol. Pharmacol.* **66,** 312–321
19. Mercier, J. F., Salahpour, A., Angers, S., Breit, A., and Bouvier, M. (2002) *J. Biol. Chem.* **277,** 44925–44931
20. Lowry, O. H., Rosebrough, N. J., Farr, A. L., and Randall, R. J. (1951) *J. Biol. Chem.* **193,** 265–275
21. Schlador, M. L., Grubbs, R. D., and Nathanson, N. M. (2000) *J. Biol. Chem.* **275,** 23295–23302
22. Halvorsen, S. W., and Nathanson, N. M. (1981) *J. Biol. Chem.* **256,** 7941–7948
23. McKinnon, L. A., and Nathanson, N. M. (1995) *J. Biol. Chem.* **270,** 20636–20642
24. Veatch, W., and Stryer, L. (1977) *J. Mol. Biol.* **113,** 89–102
25. Ayoub, M. A., Couturier, C., Lucas-Meunier, E., Angers, S., Fossier, P., Bouvier, M., and Jockers, R. (2002) *J. Biol. Chem.* **277,** 21522–21528
26. Oki, T., Takagi, Y., Inagaki, S., Taketo, M. M., Manabe, T., Matsui, M., and Yamada, S. (2005) *Mol. Brain Res.* **133,** 6–11
27. Kurogouchi, F., Nakane, T., Furukawa, Y., Hirose, M., Inada, Y., and Chiba, S. (2002) *Clin. Exp. Pharmacol. Physiol.* **29,** 666–672
28. Ostrom, R. S., and Ehlert, F. J. (1997) *J. Pharmacol. Exp. Ther.* **280,** 189–199
29. Zeng, F. Y., and Wess, J. (2000) *Neuropsychopharmacology* **23,** S19–S31
30. Dann, C. E., Hsieh, J.-C., Rattner, A., Sharma, D., Nathans, J., and Leahy, D. J. (2001) *Nature* **412,** 86–90
31. Wang, D., Sun, X., Bohn, L. M., and Sadée, W. (2005) *Mol. Pharmacol.* **67,** 2173–2184
32. Canals, M., Burgueño, J., Marcellino, D., Cabello, N., Canela, E. I., Mallol, J., Agnati, L., Ferré, S., Bouvier M., Fuxe, K., Ciruela, F., Lluis, C., and Franco, F. (2004) *J. Neurochem.* **88,** 726–734
33. Park, P. S.-H., and Wells, J. W. (2003) *Biochemistry* **42,** 12960–12971
34. Park, P. S.-H., and Wells, J. W. (2004) *J. Neurochem.* **90,** 537–548
35. Maggio, R., Barbier, P., Colelli, A., Salvadori, F., Demontis, G., and Corsini, G. U. (1999) *J. Pharmacol. Exp. Ther.* **291,** 251–257
36. Novi, F., Stanasila, L., Giorgi, F., Corsini, G. U., Cotecchia, S., and Maggio, R. (2005) *J. Biol. Chem.* **280,** 19768–19776
37. Griffin, M. T., Hsu, J. C.-H., Shehnaz, D., and Elhert, F. J. (2003) *Biochem. Pharmacol.* **65,** 1227–1241
38. Gouldson, P. R., Higgs, C., Smith, R. E., Dean, M. K., Gkoutos, G. V., and Reynolds, C. A. (2000) *Neuropsychopharmacology* **23,** S60–S77
39. Breit, A., Lagacé, M., and Bouvier, M. (2004) *J. Biol. Chem.* **279,** 28756–28765
40. Ramsay, D., Carr, I. C., Pediani, J., López-Giménez, J. F., Thurlow, R., Fidock, M., and Milligan, G. (2004) *Mol. Pharmacol.* **66,** 228–239
41. Novi, F., Scarselli, M., Corsini, G. U., and Maggio, R. (2004) *J. Biol. Chem.* **279,** 7476–7486
42. Goldman, P. S., and Nathanson, N. M. (1994) *J. Biol. Chem.* **269,** 15640–15645
43. Goldman, P. S., Schlador, M. L., Shapiro, R. A., and Nathanson, N. M. (1996) *J. Biol. Chem.* **271,** 4215–4222
44. Tsuga, H., Kameyama, K., Haga, T., Lameh, J., and Sadée, W. (1998) *J. Biol. Chem.* **273,** 5323–5330
45. Lameh, J., Philip, M., Sharma, Y. K., Moro, O., Ramachandran, J., and Sadée, W. (1992) *J. Biol. Chem.* **267,** 13406–13412
46. Roseberry, A., and Hosey, M. M. (1999) *J. Biol. Chem.* **274,** 33671–33676
47. Schlador, M. L., and Nathanson, N. M. (1997) *J. Biol. Chem.* **272,** 18882–18890